

Nuclear effects in Drell-Yan pair production in high-energy pA collisions

Eduardo Basso,^{1,*} Victor P. Goncalves,^{2,3,†} Michal Krelina,^{4,‡} Jan Nemchik,^{4,5,§} and Roman Pasechnik^{2,¶}

¹*Instituto de Física, Universidade Federal do Rio de Janeiro,
 Caixa Postal 68528, Rio de Janeiro, RJ 21941-972, Brazil*

²*Department of Astronomy and Theoretical Physics, Lund University, SE-223 62 Lund, Sweden*

³*High and Medium Energy Group, Instituto de Física e Matemática,
 Universidade Federal de Pelotas, Pelotas, RS, 96010-900, Brazil*

⁴*Czech Technical University in Prague, FNSPE, Břehová 7, 11519 Prague, Czech Republic*

⁵*Institute of Experimental Physics SAS, Watsonova 47, 04001 Košice, Slovakia*

The Drell-Yan (DY) process of dilepton pair production off nuclei is not affected by final state interactions, energy loss or absorption. A detailed phenomenological study of this process is thus convenient for investigation of the onset of initial-state effects in proton-nucleus (pA) collisions. In this paper, we present a comprehensive analysis of the DY process in pA interactions at RHIC and LHC energies in the color dipole framework. We analyse several effects affecting the nuclear suppression, $R_{pA} < 1$, of dilepton pairs, such as the saturation effects, restrictions imposed by energy conservation (the initial-state effective energy loss) and the gluon shadowing, as a function of the rapidity, invariant mass of dileptons and their transverse momenta p_T . In this analysis, we take into account besides the γ^* also the Z^0 contribution to the production cross section, thus extending the predictions to large dilepton invariant masses. Besides the nuclear attenuation of produced dileptons at large energies and forward rapidities emerging due to the onset of shadowing effects, we predict a strong suppression at large p_T , dilepton invariant masses and Feynman x_F caused by the Initial State Interaction effects in kinematic regions where no shadowing is expected. The manifestations of nuclear effects are investigated also in terms of the correlation function in azimuthal angle between the dilepton pair and a forward pion $\Delta\phi$ for different energies, dilepton rapidities and invariant dilepton masses. We predict that the characteristic double-peak structure of the correlation function around $\Delta\phi \simeq \pi$ arises for very forward pions and large-mass dilepton pairs.

I. INTRODUCTION

During the last two decades, a series of theoretical and experimental studies of particle production in heavy ion collisions (HICs) at Relativistic Heavy Ion Collider (RHIC) and Large Hadrons Collider (LHC) energies has been performed. These results provided us with various sources of information on properties of the hot and dense matter (Quark Gluon Plasma) formed in these collisions. Although several issues still remain open, those are mainly related to a description of nuclear effects related to the initial-state formation before it interacts with a nuclear target, as well as to the parton propagation in a nuclear medium. In this context, the phenomenological studies of hard processes in proton-nucleus (pA) collisions can provide us with an additional quantitative information about various nuclear effects expected also in HICs. This can help us to disentangle between the medium effects of different types and constrain their relative magnitudes and contributions [1].

A key feature of the Drell-Yan (DY) process is the absence of final state interactions and fragmentation associated with an energy loss or absorption phenomena. For this reason, the DY process can be considered as a very clean probe for the Initial State Interaction (ISI) effects [2]. In practice, this process can be used as a convenient tool in studies of the Quantum Chromodynamics (QCD) at high energies, in particular, the saturation effects expected to

*Electronic address: eduardo.basso@thep.lu.se

†Electronic address: victor.goncalves@thep.lu.se

‡Electronic address: michal.krelina@jfifi.cvut.cz

§Electronic address: nemcik@saske.sk

¶Electronic address: roman.pasechnik@thep.lu.se

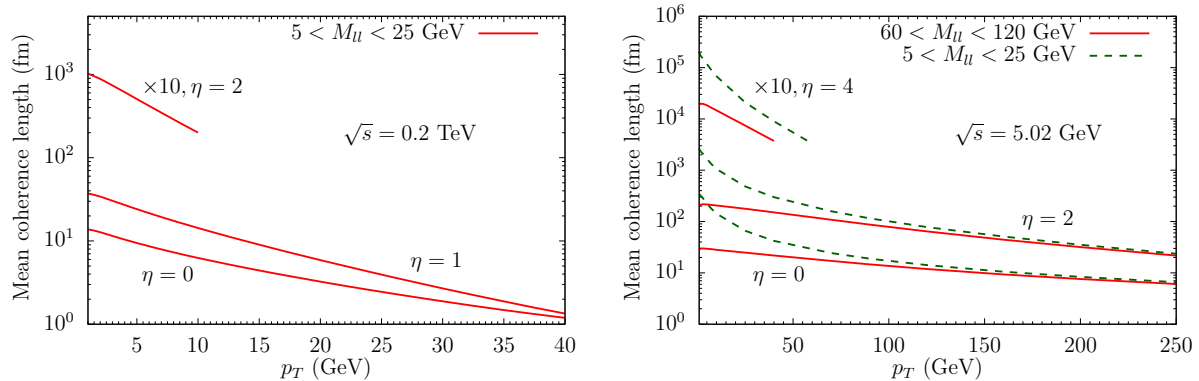


FIG. 1: (Color online) The mean coherence length l_c of the DY reaction in pA collisions at RHIC and LHC energies for different dilepton rapidities and invariant mass ranges.

determine the initial conditions in hadronic collisions as well as the initial-state energy loss due to the projectile quark propagation in the nuclear medium before it experiences a hard scattering.

In the present paper, we study the DY process on nuclear targets at high energies using the color dipole approach [3–12], which is known to give as precise prediction for the DY cross section as the Next-to-Leading-Order (NLO) collinear factorization framework and allows to include naturally the coherence effects in nuclear collisions. Moreover, the color dipole formalism provides a straightforward generalisation of the DY process description from the proton-proton to proton-nucleus collisions and is thus suitable for studies of nuclear effects directly accessing the impact parameter dependence of nuclear shadowing and nuclear broadening – the critical information which is not available in the parton model.

In contrast to the conventional parton model where the dilepton production process is typically viewed as the parton annihilation in the center of mass (c.m.) frame, in the color dipole approach operating in the target rest frame the same process looks as a bremsstrahlung of a γ^*/Z^0 boson off a projectile quark. In pA collisions assuming the high energy limit, the projectile quark probes a dense gluonic field in the target and the nuclear shadowing leads to a nuclear modification of the transverse momentum distribution of the DY production cross section. The onset of shadowing effects is controlled by the coherence length, which can be interpreted as the mean lifetime of γ^*/Z^0 -quark fluctuations, and is given by

$$l_c = \frac{1}{x_2 m_N} \frac{(M_{ll}^2 + p_T^2)(1 - \alpha)}{\alpha(1 - \alpha)M_{ll}^2 + \alpha^2 m_f^2 + p_T^2}, \quad (1)$$

where M_{ll} is the dilepton invariant mass and p_T its transverse momentum. Moreover, α is the fraction of the light-cone momentum of the projectile quark carried out by the gauge boson. As demonstrated in Fig. 1, in the RHIC and LHC kinematic regions, the coherence length exceeds the nuclear radius R_A , $l_c \gtrsim R_A$, which implies that the long coherence length (LCL) limit can be safely used in practical calculations of the DY cross section in pA collisions.

Besides the quark shadowing effects naturally accounted for in the dipole picture, one should also take into account the nuclear effects due to multiple rescattering of initial-state projectile partons (ISI effects) in a medium before a hard scattering. The latter are important close to the kinematic limits, e.g. at large Feynman $x_F \rightarrow 1$ and $x_T = 2p_T/\sqrt{s} \rightarrow 1$ (\sqrt{s} is the collision energy in c.m. frame), due to restrictions imposed by energy conservation. In the present paper, we take into account also non-linear QCD effects, which are amplified in nuclear collisions and related to multiple scatterings of the higher Fock states containing gluons in the dipole-target interactions. They generate the gluon shadowing effects effective at small Bjorken x in the target and large rapidity values.

In our study, all the basic ingredients for the DY nuclear production cross section (such as the dipole cross section parameterisations and Parton Distribution Functions (PDFs)) have been determined from other processes. Consequently, our predictions are parameter-free and should be considered as an important test for the onset of distinct nuclear effects. Note that the nuclear DY process mediated by a virtual photon has been already studied within the color dipole framework by several authors (see e.g. Refs. [7–9]). However, the results of this paper represent a further step updating and improving the previous analyses in the literature providing new predictions for the transverse momentum, dilepton invariant mass and rapidity distributions of the nuclear DY production cross section at RHIC and LHC energies as well as in comparison to the most recent data. Besides, the effects of quantum coherence at large energies including the gluon shadowing as a leading-twist shadowing correction as well as an additional contribution

of the Z^0 boson and γ^*/Z^0 interference are incorporated. Moreover, the impact of the effective initial state energy loss effects on the DY nuclear production cross section is studied for the first time. We also investigate nuclear effects providing a detailed analysis of the azimuthal correlation between the produced DY pair and a forward pion taking into account the Z^0 boson contribution in addition to virtual photon, generalising thus the results presented in Ref. [13].

This paper is organized as follows. In the Section II, we present a brief overview of gauge boson production in the color dipole framework. Moreover, we discuss in detail the saturation effects, gluon shadowing and initial-state energy loss effects included in the analysis. Section III is devoted to predictions for the dilepton invariant mass, rapidity and transverse momentum distributions of the DY nuclear production cross sections in comparison with the available data. The onset of various nuclear effects is estimated in the LCL limit and the predictions for the nucleus-to-nucleon ratio, $R_{pA} = \sigma_{pA}/A\sigma_{pp}$ ¹, of the DY production cross sections are presented. The latter can be verified in the future by experiments at RHIC and LHC. Furthermore, the azimuthal correlation function between the produced dilepton and a pion is evaluated for pA collisions at RHIC and LHC for different dilepton invariant masses including the high-mass region. Finally, in Section IV we summarise our main conclusions.

II. DRELL-YAN PROCESS IN HADRON-NUCLEUS COLLISIONS

A. DY nuclear cross section

The color dipole formalism is treated in the target rest frame where the process of DY pair production can be viewed as a radiation of gauge bosons $G^* = \gamma^*/Z^0$ by a projectile quark (see e.g. Ref. [10, 12]). Assuming only the lowest $|qG^*\rangle$ Fock component, the cross section for the inclusive gauge boson production with invariant mass $M_{l\bar{l}}$ and transverse momentum p_T can be expressed in terms of the projectile quark (antiquark) densities q_f (\bar{q}_f) at momentum fraction x_q and the quark-nucleus cross section as follows (see e.g. Refs. [7, 12]),

$$\frac{d\sigma(pA \rightarrow G^*X)}{d^2p_T d\eta} = J(\eta, p_T) \frac{x_1}{x_1 + x_2} \sum_f \sum_{\lambda_G=L,T} \int_{x_1}^1 \frac{d\alpha}{\alpha^2} [q_f(x_q, \mu_F^2) + \bar{q}_f(x_q, \mu_F^2)] \frac{d\sigma_{\lambda_G}^f(qA \rightarrow qG^*X)}{d(\ln \alpha) d^2p_T}, \quad (2)$$

where

$$J(\eta, p_T) \equiv \frac{dx_F}{d\eta} = \frac{2}{\sqrt{s}} \sqrt{M_{l\bar{l}}^2 + p_T^2} \cosh(\eta) \quad (3)$$

is the Jacobian of transformation between the Feynman variable $x_F = x_1 - x_2$ and pseudorapidity η of the virtual gauge boson G^* , $x_q = x_1/\alpha$, where α is the fraction of the light-cone momentum of the projectile quark carried out by the gauge boson, and $\mu_F^2 = p_T^2 + (1 - x_1)M_{l\bar{l}}^2$ is the factorization scale in quark PDFs. As in Ref. [12] we take $\mu_F \simeq M_{l\bar{l}}$, for simplicity.

The transverse momentum distribution in Eq. (2) of the gauge boson G^* bremsstrahlung in quark-nucleus interactions can be obtained by a generalization of the well-known formulas for the photon bremsstrahlung from Refs. [5, 7, 8]. Then the corresponding differential cross section for a given incoming quark of flavour f reads,

$$\begin{aligned} \frac{d\sigma_{T,L}^f(qA \rightarrow qG^*X)}{d(\ln \alpha) d^2p_T} &= \frac{1}{(2\pi)^2} \sum_{\text{quark pol.}} \int d^2\rho_1 d^2\rho_2 \exp[i\mathbf{p}_T \cdot (\boldsymbol{\rho}_1 - \boldsymbol{\rho}_2)] \Psi_{T,L}^{\mathcal{V}-\mathcal{A}}(\alpha, \boldsymbol{\rho}_1, m_f) \Psi_{T,L}^{\mathcal{V}-\mathcal{A},*}(\alpha, \boldsymbol{\rho}_2, m_f) \\ &\times \frac{1}{2} [\sigma_{q\bar{q}}^A(\alpha\boldsymbol{\rho}_1, x_2) + \sigma_{q\bar{q}}^A(\alpha\boldsymbol{\rho}_2, x_2) - \sigma_{q\bar{q}}^A(\alpha|\boldsymbol{\rho}_1 - \boldsymbol{\rho}_2|, x_2)], \end{aligned} \quad (4)$$

where $x_2 = x_1 - x_F$ and $\boldsymbol{\rho}_{1,2}$ are the quark- G^* transverse separations in the total radiation amplitude and its conjugated counterpart, respectively. Assuming that the projectile quark is unpolarized, the vector $\Psi^{\mathcal{V}}$ and axial-vector $\Psi^{\mathcal{A}}$ wave functions in Eq. (4) are not correlated such that

$$\begin{aligned} &\sum_{\text{quark pol.}} \Psi_{T,L}^{\mathcal{V}-\mathcal{A}}(\alpha, \boldsymbol{\rho}_1, m_f) \Psi_{T,L}^{\mathcal{V}-\mathcal{A},*}(\alpha, \boldsymbol{\rho}_2, m_f) = \\ &= \Psi_{T,L}^{\mathcal{V}}(\alpha, \boldsymbol{\rho}_1, m_f) \Psi_{T,L}^{\mathcal{V},*}(\alpha, \boldsymbol{\rho}_2, m_f) + \Psi_{T,L}^{\mathcal{A}}(\alpha, \boldsymbol{\rho}_1, m_f) \Psi_{T,L}^{\mathcal{A},*}(\alpha, \boldsymbol{\rho}_2, m_f), \end{aligned} \quad (5)$$

¹ Here A represents the atomic mass number of the nuclear target

where the averaging over the initial and summation over final quark helicities is performed and the quark flavour dependence comes only via the projectile quark mass m_f . The corresponding wave functions $\Psi_{T,L}^{\nu-A}(\alpha, \rho)$ can be found in Ref. [10].

Our goal is to evaluate the DY production cross section in pA collisions at high energies and a large mass number A of the nuclear target. This regime is characterised by a limitation on the maximum phase-space parton density that can be reached in the hadron wave function (parton saturation) [14]. The transition between the linear and non-linear regimes of QCD dynamics is typically specified by a characteristic energy-dependent scale called the saturation scale Q_s^2 , where the variable s denotes c.m. energy squared of the collision. Such saturation effects are expected to be amplified in nuclear collisions since the nuclear saturation scale $Q_{s,A}^2$ is expected to be enlarged with respect to the nucleon one $Q_{s,p}^2$ by roughly a factor of $A^{1/3}$.

In general, the dipole-nucleus cross section $\sigma_{q\bar{q}}^A(\rho, x)$ can be written in terms of the forward dipole-nucleus scattering amplitude $\mathcal{N}^A(\rho, x, \mathbf{b})$ as follows,

$$\sigma_{q\bar{q}}^A(\rho, x) = 2 \int d^2\mathbf{b} \mathcal{N}^A(\rho, x, \mathbf{b}). \quad (6)$$

At high energies, the evolution of $\mathcal{N}^A(x, \mathbf{r}, \mathbf{b})$ in rapidity $Y = \ln(1/x)$ is given, for example, within the Color Glass Condensate (CGC) formalism [15], in terms of an infinite hierarchy of equations known as so called Balitsky-JIMWLK equations [15, 16], which reduces in the mean field approximation to the Balitsky-Kovchegov (BK) equation [16, 17]. In recent years, several groups have studied the solution of the BK equation taking into account the running coupling corrections to the evolution kernel. However, these analyses have assumed the translational invariance approximation, which implies that $\mathcal{N}^A(\rho, x, \mathbf{b}) = \mathcal{N}^A(\rho, x) S(\mathbf{b})$ and $\sigma_{q\bar{q}}^A(\rho, x, \mathbf{b}) = \sigma_0 \mathcal{N}(\rho, x)$, where $\mathcal{N}(\rho, x)$ is a partial dipole amplitude on a nucleon, and σ_0 is the normalization of the dipole cross section fitted to the data. Basically, they disregard the impact parameter dependence. Unfortunately, the impact-parameter dependent numerical solutions of the BK equation are very difficult to obtain [18]. Moreover, the choice of the impact-parameter profile of the dipole amplitude entails intrinsically nonperturbative physics, which is beyond the QCD weak coupling approach of the BK equation. In what follows, we explore an alternative path and employ the available phenomenological models, which explicitly incorporate an expected b -dependence of the scattering amplitude.

B. Models for the dipole cross section

As in our previous studies [19–24], we work in the LCL limit and employ the model initially proposed in Ref. [25] which includes the impact parameter dependence in the dipole-nucleus amplitude and describes the experimental data on the nuclear structure function (for more details, see Ref. [19, 26]). In particular, this model enables us to incorporate the shadowing effects via a simple eikonalization of the standard dipole-nucleon cross section $\sigma_{q\bar{q}}(\rho, x)$ such that the forward dipole-nucleus amplitude in Eq. (6) is given by

$$\mathcal{N}^A(\rho, x, \mathbf{b}) = 1 - \exp\left(-\frac{1}{2} T_A(\mathbf{b}) \sigma_{q\bar{q}}(\rho, x)\right), \quad (7)$$

where $T_A(\mathbf{b})$ is the nuclear profile (thickness) function, which is normalized to the mass number A and reads

$$T_A(\mathbf{b}) = \int_{-\infty}^{\infty} \rho_A(\mathbf{b}, z) dz. \quad (8)$$

Here $\rho_A(\mathbf{b}, z)$ represents the nuclear density function defined at the impact parameter \mathbf{b} and the longitudinal coordinate z . In our calculations we used realistic parametrizations of $\rho_A(\mathbf{b}, z)$ from Ref. [27]. The eikonal formula (7) based upon the Glauber-Gribov formalism [28] resums the multiple elastic rescattering diagrams of the $q\bar{q}$ dipole in a nucleus in the high-energy limit. The eikonalisation procedure is justified in the LCL regime where the transverse separation ρ of partons in the multiparton Fock state of the photon is frozen during propagation through the nuclear matter and becomes an eigenvalue of the scattering matrix.

For the numerical analysis of the nuclear DY observables, we need to specify a reliable parametrisation for the dipole-proton cross section. In recent years, several groups have constructed a number of viable phenomenological models based on saturation physics and fits to the HERA and RHIC data (see e.g. Refs. [29–41]).

As in our previous study of the DY process in pp collisions [12], in order to estimate theoretical uncertainty in our analysis, in what follows, we consider several phenomenological models for the dipole cross section $\sigma_{q\bar{q}}$ which take into account the DGLAP evolution as well as the saturation effects.

The first one is the model proposed in Ref. [38], where the dipole cross section is given by

$$\sigma_{q\bar{q}}(\boldsymbol{\rho}, x) = \sigma_0 \left[1 - \exp \left(-\frac{\pi^2}{\sigma_0 N_c} \rho^2 \alpha_s(\mu^2) xg(x, \mu^2) \right) \right], \quad (9)$$

where $N_c = 3$ is the number of colors, $\alpha_s(\mu^2)$ is the strong coupling constant at μ scale, which is related to the dipole size ρ as $\mu^2 = C/\rho^2 + \mu_0^2$ with C , μ_0 and σ_0 parameters fitted to the HERA data. Moreover, in this model the gluon density evolves according to DGLAP equation [42] accounting for gluon splittings only,

$$\frac{\partial xg(x, \mu^2)}{\partial \ln \mu^2} = \frac{\alpha_s(\mu^2)}{2\pi} \int_x^1 dz P_{gg}(z) \frac{x}{z} g\left(\frac{x}{z}, \mu^2\right), \quad (10)$$

where the gluon density at initial scale μ_0^2 is parametrized as [38]

$$xg(x, \mu_0^2) = A_g x^{-\lambda_g} (1-x)^{5.6}. \quad (11)$$

The set of best fit values of the model parameters reads: $A_g = 1.2$, $\lambda_g = 0.28$, $\mu_0^2 = 0.52 \text{ GeV}^2$, $C = 0.26$ and $\sigma_0 = 23 \text{ mb}$. In what follows we denote by BGBK the predictions for the DY observables obtained using Eq. (9) as an input in calculations of the dipole-nucleus scattering amplitude.

The model proposed in Ref. [38] was generalised in Ref. [35] in order to take into account the impact parameter dependence of the dipole-proton cross section and to describe the exclusive observables at HERA. In this model, the corresponding dipole-proton cross section is given by

$$\sigma_{q\bar{q}}(\boldsymbol{\rho}, x) = 2 \int d^2 b_p \left[1 - \exp \left(-\frac{\pi^2}{2N_c} \rho^2 \alpha_s(\mu^2) xg(x, \mu^2) T_G(\mathbf{b}_p) \right) \right] \quad (12)$$

with the DGLAP evolution of the gluon distribution given by Eq. (10). The Gaussian impact parameter dependence is given by $T_G(\mathbf{b}_p) = (1/2\pi B_G) \exp(-b_p^2/2B_G)$, where B_G is a free parameter extracted from the t -dependence of the exclusive electron-proton (ep) data. The parameters of this model were updated in Ref. [40] by fitting to the recent high precision HERA data [43] providing the following values: $A_g = 2.373$, $\lambda_g = 0.052$, $\mu_0^2 = 1.428 \text{ GeV}^2$, $B_G = 4.0 \text{ GeV}^2$ and $C = 4.0$. Hereafter, we will denote as IP-SAT the resulting predictions obtained using Eq. (12) as an input in calculations of \mathcal{N}^A , Eq. (7).

For comparison with the previous results existing in the literature, we also consider the Golec-Biernat-Wusthoff (GBW) model [29] based upon a simplified saturated form

$$\sigma_{q\bar{q}}(\boldsymbol{\rho}, x) = \sigma_0 \left(1 - e^{-\frac{\rho^2 Q_s^2(x)}{4}} \right) \quad (13)$$

with the saturation scale

$$Q_s^2(x) = Q_0^2 \left(\frac{x_0}{x} \right)^\lambda, \quad (14)$$

where the model parameters $Q_0^2 = 1 \text{ GeV}^2$, $x_0 = 4.01 \times 10^{-5}$, $\lambda = 0.277$ and $\sigma_0 = 29 \text{ mb}$ were obtained from the fit to the DIS data accounting for a contribution of the charm quark.

Finally, we also consider the running coupling solution of the BK equation for the partial dipole amplitude obtained in the Ref. [44] using the GBW model as an initial condition such that $\sigma_{q\bar{q}}^p(\boldsymbol{\rho}, x) = \sigma_0 \mathcal{N}^p(\boldsymbol{\rho}, x)$ where the normalisation σ_0 is fitted to the HERA data.

C. Gluon shadowing corrections

In the LHC energy range the eikonal formula for the LCL regime, Eq. (7), is not exact. Besides the lowest $|qG^*\rangle$ Fock state, where $G^* = \gamma^*/Z^0$, one should include also the higher Fock components containing gluons, e.g. $|qG^*g\rangle$, $|qG^*gg\rangle$, etc. They cause an additional suppression known as the gluon shadowing (GS). Such high LHC energies allow so to activate the coherence effects also for these gluon fluctuations, which are heavier and consequently have a shorter coherence length than lowest Fock component $|qG^*\rangle$. The corresponding suppression factor R_G , as the ratio of the gluon densities in nuclei and nucleon, was derived in Ref. [45] using the Green function technique through the

calculation of the inelastic correction $\Delta\sigma_{tot}(q\bar{q}g)$ to the total cross section $\sigma_{tot}^{\gamma^*A}$, related to the creation of a $|q\bar{q}g\rangle$ intermediate Fock state

$$R_G(x, Q^2, \mathbf{b}) \equiv \frac{xg_A(x, Q^2, \mathbf{b})}{A \cdot xg_p(x, Q^2)} \approx 1 - \frac{\Delta\sigma_{tot}(q\bar{q}g)}{\sigma_{tot}^{\gamma^*A}}. \quad (15)$$

GS corrections are included in calculations replacing $\sigma_{q\bar{q}}^N(\boldsymbol{\rho}, x) \rightarrow \sigma_{q\bar{q}}^N(\boldsymbol{\rho}, x) R_G(x, Q^2, \mathbf{b})$. They lead to additional nuclear suppression in production of DY pairs at small Bjorken $x = x_2$ in the target. In Fig. 2 (left panel) we present our results for the x dependence of the ratio $R_G(x, Q^2, \mathbf{b})$ for different values of the impact parameter b . As expected, the magnitude of the shadowing corrections decreases at large values of b . In the right panel we present our predictions for the b -integrated nuclear ratio $R_G(x, Q^2)$ for different values of the hard scale Q^2 . This figure shows a not very strong onset of GS, which was confirmed by the NLO global analyses of DIS data [46]. A weak Q^2 dependence of GS demonstrates that GS is a leading twist effect, with $R_G(x, Q^2)$ approaching unity only very slowly (logarithmically) as $Q^2 \rightarrow \infty$.

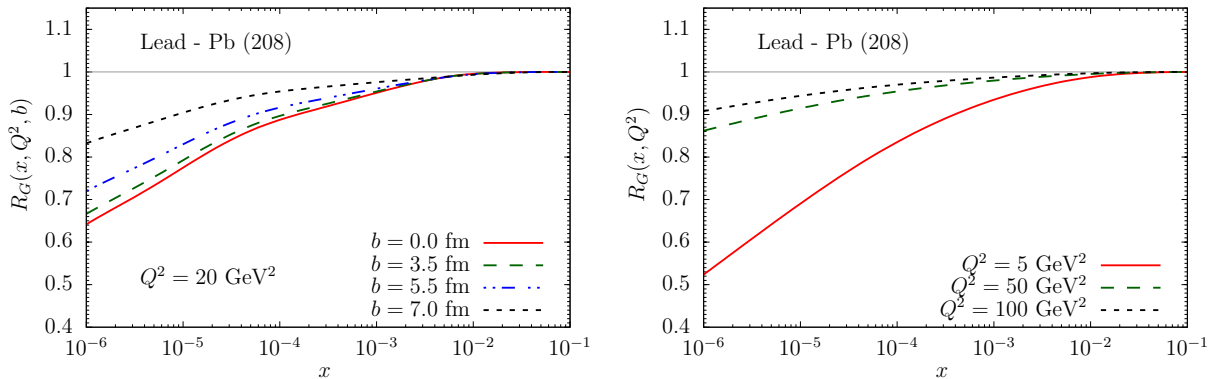


FIG. 2: (Color online) Left panel: The x -dependence of the ratio $R_G(x, Q^2, \mathbf{b})$ for different values of the impact parameter. Right panel: The x -dependence of the b -integrated ratio $R_G(x, Q^2)$ for distinct values of the hard scale Q^2 .

D. Effective energy loss

The effective initial-state energy loss (ISI effects) is expected to suppress noticeably the nuclear cross section when reaching the kinematical limits,

$$x_L = \frac{2p_L}{\sqrt{s}} \rightarrow 1, \quad x_T = \frac{2p_T}{\sqrt{s}} \rightarrow 1.$$

Correspondingly, a proper variable which controls this effect is $\xi = \sqrt{x_L^2 + x_T^2}$. The magnitude of suppression was evaluated in Ref. [47]. It was found within the Glauber approximation that each interaction in the nucleus leads to a suppression factor $S(\xi) \approx 1 - \xi$. Summing up over the multiple initial state interactions in a pA collision at impact parameter b , one arrives at a nuclear ISI-modified PDF

$$q_f(x, Q^2) \Rightarrow q_f^A(x, Q^2, b) = C_v q_f(x, Q^2) \frac{e^{-\xi\sigma_{\text{eff}}T_A(b)} - e^{-\sigma_{\text{eff}}T_A(b)}}{(1 - \xi)(1 - e^{-\sigma_{\text{eff}}T_A(b)})}. \quad (16)$$

Here, $\sigma_{\text{eff}} = 20$ mb is the effective hadronic cross section controlling the multiple interactions. The normalisation factor C_v is fixed by the Gottfried sum rule (for more details, see Ref. [47]). It was found that such an additional nuclear suppression emerging due to the ISI effects represents an energy independent feature common for all known reactions experimentally studied so far, with any leading particle (hadrons, Drell-Yan dileptons, charmonium, etc). In particular, such a suppression was indicated at midrapidity, $y = 0$, and at large p_T by the PHENIX data [48] on π^0 production in central dAu collisions and on direct photon production in central $AuAu$ collisions [49], where no shadowing is expected since the corresponding Bjorken $x = x_2$ in the target is large. Besides large p_T -values, the same mechanism of nuclear attenuation is effective also at forward rapidities (large Feynman x_F), where we expect a much stronger onset of nuclear suppression as was demonstrated by the BRAHMS and STAR data [50]. In our case, we predict that the ISI effects induce a significant suppression of the DY nuclear cross section at large dilepton p_T , dilepton invariant mass and at forward rapidities as one can see in the next Section.

III. RESULTS

In what follows, we present our predictions for the DY pair production cross section in the process $pA \rightarrow \gamma^*/Z^0 \rightarrow l\bar{l}$ obtained within the color dipole formalism and taking into account the medium effects discussed in the previous Section. Following Ref. [29], we use the quark mass values to be $m_u = m_d = m_s = 0.14$ GeV, $m_c = 1.4$ GeV and $m_b = 4.5$ GeV. Moreover, we take the factorisation scale μ_F defined above to be equal to the dilepton invariant mass, $M_{l\bar{l}}$, and employ the CT10 NLO parametrisation for the projectile quark PDFs [51] (both sea and valence quarks are included). As was demonstrated in Refs. [12, 52], there is a little sensitivity of DY predictions on PDF parameterisation in pp collisions at high energies so we do not vary the projectile quark PDFs.

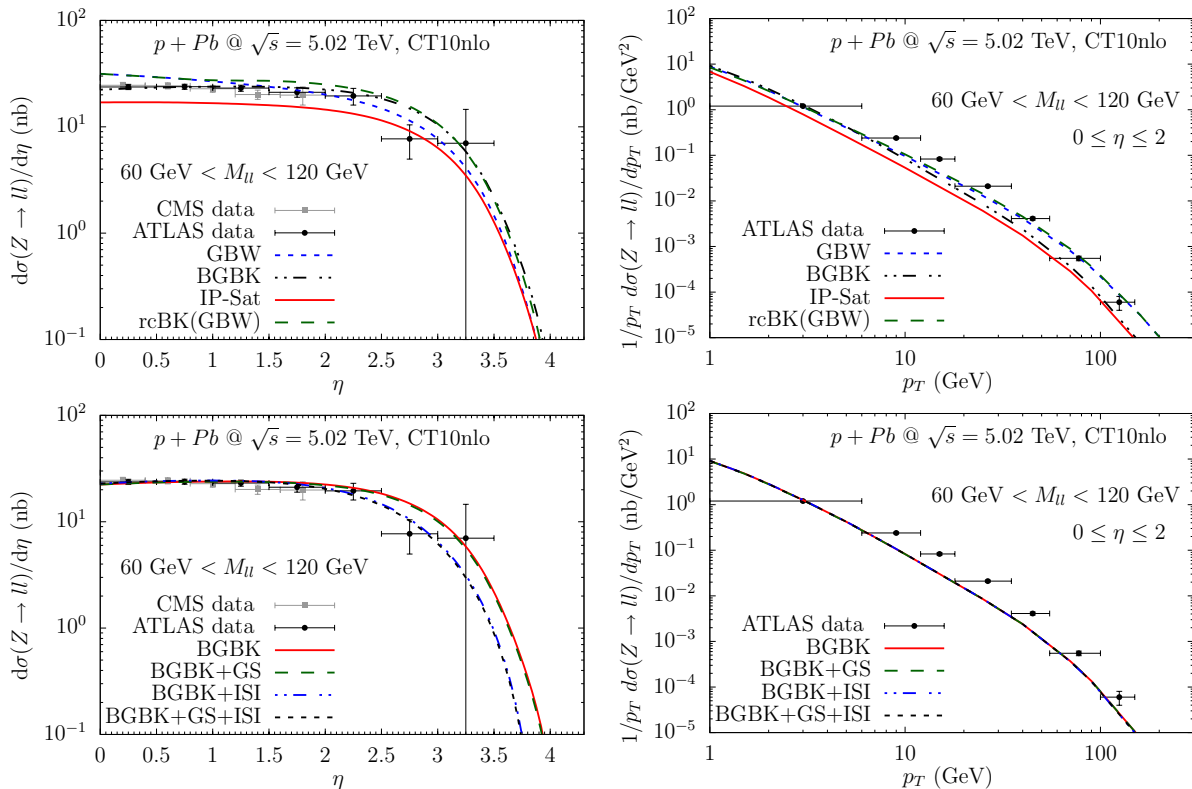


FIG. 3: (Color online) The dipole model predictions for the DY nuclear cross sections at large dilepton invariant masses compared to the recent experimental data from ATLAS and CMS experiments [53, 54] at c.m. collision energy $\sqrt{s} = 5.02$ TeV. The predictions obtained for several parameterisations of the dipole cross section described in the text are shown in the top panels while the effects of the gluon shadowing and the initial-state energy loss are demonstrated in the bottom panels.

In Fig. 3 we compare our predictions for the DY nuclear cross section with available LHC data [53, 54] for large invariant dilepton masses, $60 < M_{l\bar{l}} < 120$ GeV, taking into account the saturation effects. In the top panels, we test the predictions of various models for the dipole cross section comparing them with the experimental data for the rapidity and transverse momentum distributions of the DY production cross sections in pA collisions. As was already verified in Ref. [12] for DY production in pp collisions, the dipole approach works fairly well in description of the current experimental data at high energies. In particular, the BGBK model provides a consistent prediction describing the data on the rapidity distribution quite well in the full kinematical range. In the bottom panels of Fig. 3, we took the BGBK model and considered the impact of gluon shadowing corrections as well as the initial-state effective energy loss (ISI effects), Eq. (16). In the range of large dilepton invariant masses concerned, the gluon shadowing corrections are rather small since the corresponding Bjorken $x = x_2$ in the target becomes large. On the other hand, the ISI effects significantly modify the behaviour of the rapidity distribution at large $\eta > 2$. Unfortunately, the current data are not able at this moment to verify the predicted strong onset of ISI effects due to large error bars. In the case of the transverse momentum distribution for large invariant masses and $0 \leq \eta \leq 2$, the impact of both the gluon shadowing and the ISI effects is negligible.

In order to quantify the impact of the nuclear effects, in what follows, we estimate the invariant mass, rapidity and transverse momentum dependence of the nucleus-to-nucleon ratio of the DY production cross sections (nuclear

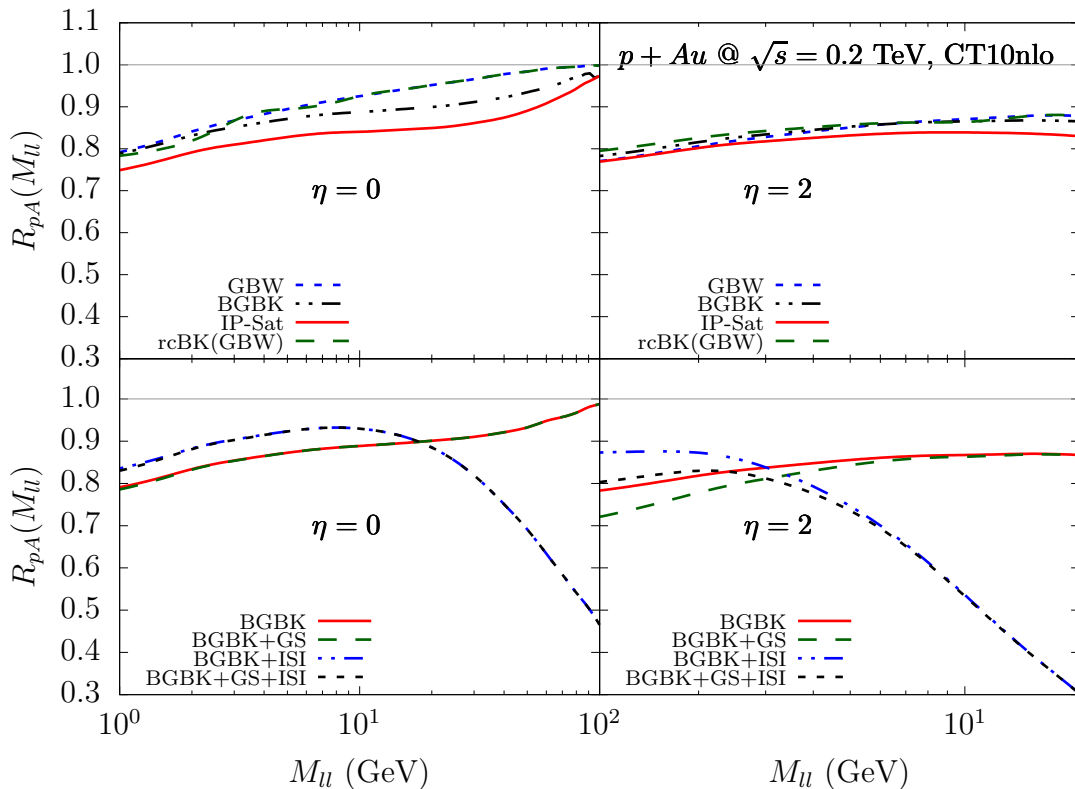


FIG. 4: (Color online) The dilepton invariant mass dependence of the nucleus-to-nucleon ratio, $R_{pA} = \sigma_{pA}^{DY} / (A \cdot \sigma_{pp}^{DY})$, of the DY production cross sections for c.m. energy $\sqrt{s} = 0.2$ TeV corresponding to RHIC experiments.

modification factor), $R_{pA} = \sigma_{pA}^{DY} / (A \cdot \sigma_{pp}^{DY})$, considering the DY process at RHIC ($\sqrt{s} = 0.2$ TeV) and LHC ($\sqrt{s} = 5.02$ TeV) energies. The color dipole predictions for the DY production cross section in pp collisions have been discussed in detail in Ref. [12]. For consistency, the numerator and denominator of the nuclear modification factor are evaluated within the same model for the dipole cross section as an input.

In Fig. 4 we present our predictions for the dilepton invariant mass dependence of the ratio $R_{pA}(M_{l\bar{l}})$ at RHIC considering both central and forward rapidities. In the top panels, we show that the dipole model predictions are almost insensitive to the parameterisations used to treat the dipole-proton interactions. The magnitude of the saturation effects decreases at large dilepton invariant masses and increases at forward rapidities. Such a behaviour is expected, since at smaller $M_{l\bar{l}}$ and at larger η one probes smaller values of the Bjorken- x_2 variable in the target. In the bottom panels of Fig. 4, we present the predictions taking into account also the GS corrections and ISI effects. As was mentioned above we predict a weak onset of GS corrections at central rapidities whereas GS leads to a significant suppression in the forward region. Besides, as expected, the impact of GS effects decreases with $M_{l\bar{l}}$ due to rise of the Bjorken x_2 -values. In contrast to that, the ISI effects become effective causing a strong nuclear suppression at large $M_{l\bar{l}}$ and/or η . This behaviour is also well understood since large dilepton invariant masses and/or rapidities correspond to large Feynman x_F leading to a stronger onset of ISI effects as follows from Eq. (16). A similar behaviour has been predicted for the LHC energy range as is shown in Fig. 5 where the impact of saturation and GS effects is even more pronounced.

In Fig. 6 we present our predictions for rapidity dependence of the nucleus-to-nucleon ratio, $R_{pA}(\eta)$, of the DY production cross sections at RHIC and LHC energies considering two ranges, ($5 < M_{l\bar{l}} < 25$ GeV) and ($60 < M_{l\bar{l}} < 120$ GeV), of dilepton invariant mass. We would like to emphasize that the onset of saturation effects reduces $R_{pA}(\eta)$ at large rapidities and have a larger impact in the small invariant mass range. For large invariant masses, we predict a reduction of $\approx 10\%$ in the R_{pPb} ratio at LHC energy. At RHIC energy we predict a weak onset of GS effects even at large $\eta > 3$. In contrast to RHIC energy range, at the LHC the GS effects lead to a significant additional suppression, modifying thus the ratio R_{pPb} especially at small dilepton invariant masses and large rapidity values. On the other hand, the onset of the ISI effects is rather strong for both RHIC and LHC kinematic regions, and becomes even stronger at forward rapidities for both invariant mass ranges. This makes the phenomenological studies of the

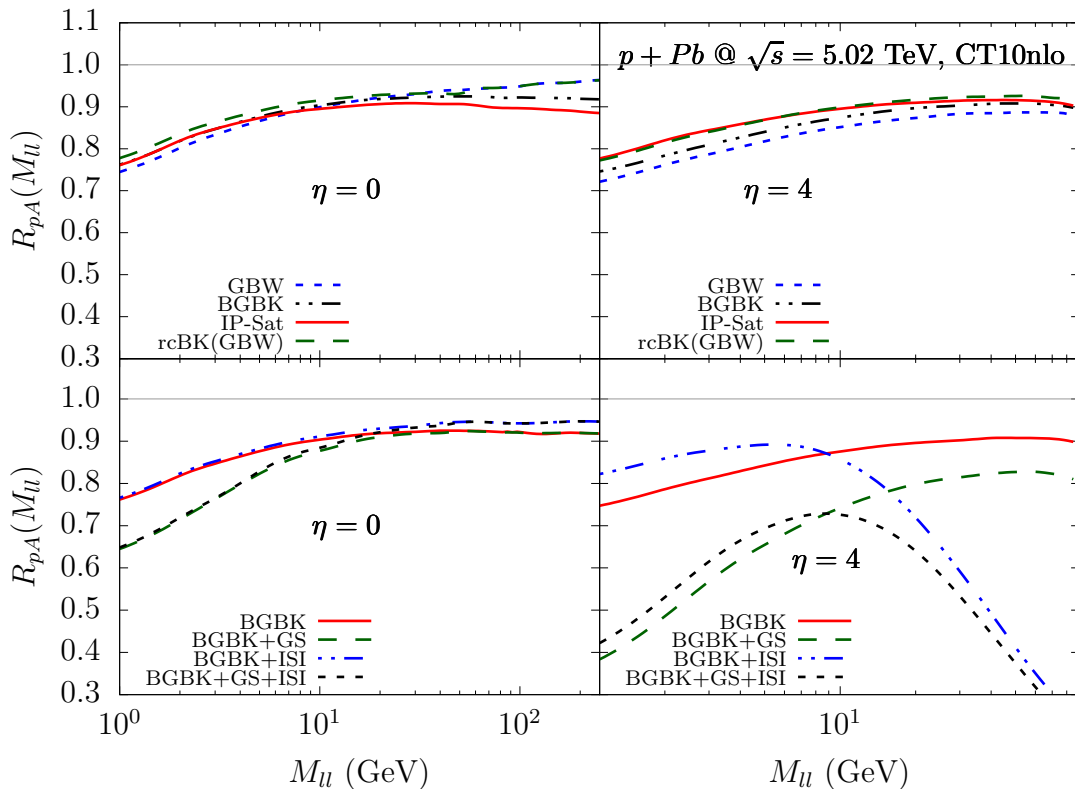


FIG. 5: (Color online) The dilepton invariant mass dependence of the nucleus-to-nucleon ratio, $R_{pA} = \sigma_{pA}^{DY} / (A \cdot \sigma_{pp}^{DY})$, of the DY production cross sections for c.m. energy $\sqrt{s} = 5.02$ TeV corresponding to LHC experiments.

rapidity dependence of R_{pA} ideal for constraining such effects.

Fig. 7 shows our predictions for the transverse momentum dependence of the nuclear modification factor, $R_{pA}(p_T)$, for the invariant mass range $5 < M_{ll} < 25$ GeV at RHIC c.m. energy $\sqrt{s} = 0.2$ TeV and two distinct pseudorapidity values $\eta = 0$ and $\eta = 1$. At large transverse momenta, the role of the saturation effects is negligibly small and can be important only at small $p_T \leq 2$ GeV. Similarly, the GS effects are almost irrelevant at RHIC energies. However, Fig. 7 clearly demonstrates a strong onset of ISI effects causing a significant suppression at large p_T , where no coherence effects are expected. In accordance with Eq. (16) and in comparison with $\eta = 0$, we predict stronger ISI effects at forward rapidities as is depicted in Fig. 7 for $\eta = 1$. Due to a significant elimination of coherence effects the study of the DY process at large p_T in pA collisions at RHIC is a very convenient tool for investigation of net ISI effects. On the other hand, at LHC energies (see Fig. 8) the manifestation of the saturation and GS effects rises at forward rapidities and becomes noticeable for $p_T \leq 10$ GeV. As was already mentioned for RHIC energies, the ISI effects cause a significant attenuation at large transverse momenta and forward rapidities, although no substantial suppression is expected in the DY process due to absence of the final state interaction, energy loss or absorption. For these reasons a study of the ratio $R_{pA}(p_T)$ also at the LHC especially at large p_T and at small invariant mass range is very effective to constrain the ISI effects.

In order to reduce the contribution of coherence effects (gluon shadowing, CGC) in the LHC kinematic region one should go to the range of large dilepton invariant masses as is shown in Fig. 9. Here we present our predictions for the ratio $R_{pPb}(p_T)$ at the LHC c.m. collision energy $\sqrt{s} = 5.02$ TeV for the range $60 < M_{ll} < 120$ GeV and several values of $\eta = 0, 2, 4$. According to expectations we have found that the saturation and GS effects turn out to be important only at small p_T and large η . Such an elimination of coherence effects taking into account larger dilepton invariant masses causes simultaneously a stronger onset of ISI effects as one can see in Fig. 9 in comparison with Fig. 8. For this reason, investigation of net ISI effects at large M_{ll} does not require such high p_T - and rapidity values, what allows to obtain the experimental data of higher statistics and consequently with smaller error bars. Fig. 9 demonstrates again a large nuclear suppression in the forward region ($\eta = 4$) over an extended range of the dilepton transverse momenta. Consequently, such an analysis of the DY nuclear cross section at forward rapidities by e.g. the LHCb Collaboration can be very useful to probe the ISI effects experimentally.

Finally, let us discuss the azimuthal correlation between the DY pair and a forward pion produced in pA collisions

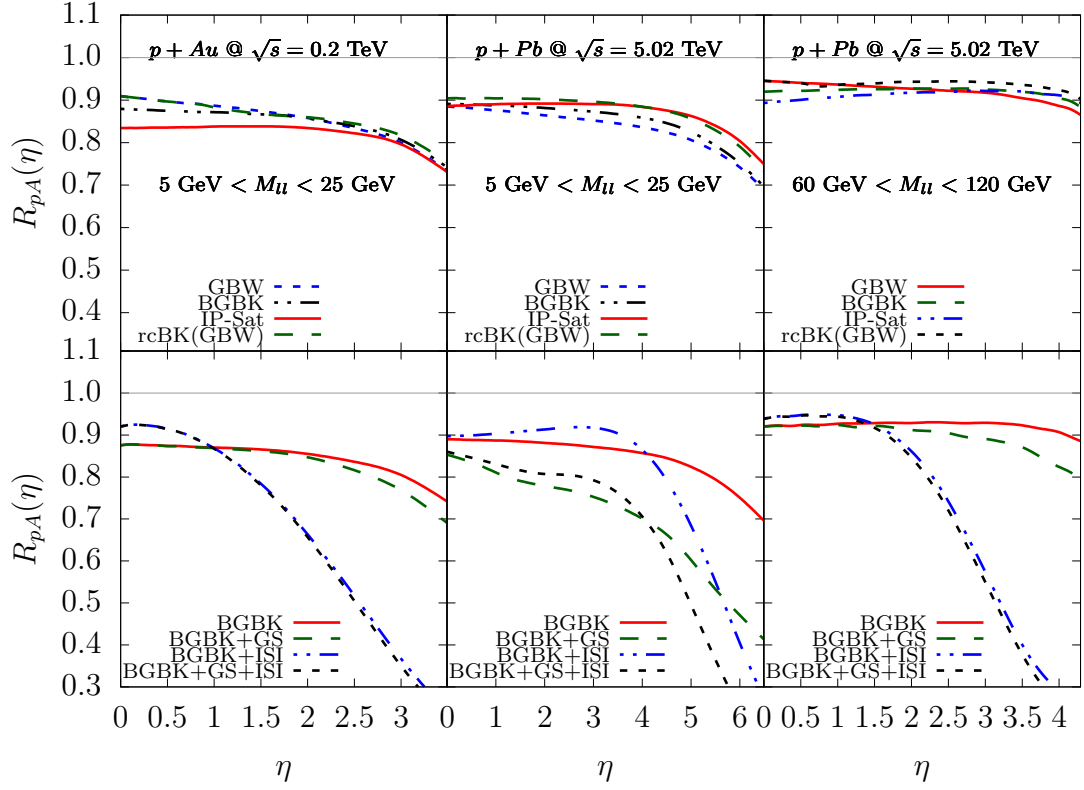


FIG. 6: (Color online) The pseudorapidity dependence of the nucleus-to-nucleon ratio, $R_{pA}(\eta)$, of the DY production cross sections at RHIC and LHC energies for two ranges ($5 < M_{l\bar{l}} < 25$ GeV) and ($60 < M_{l\bar{l}} < 120$ GeV) of dilepton invariant mass.

taking into account the Z^0 boson contribution in addition to the virtual photon as well as the saturation effects. As was discussed earlier in Refs. [12, 13, 55], the dilepton-hadron correlations can serve as an efficient probe of the initial state effects. Considering the $G^* = \gamma^*/Z_0$ boson as a trigger particle, the corresponding correlation function can be written as

$$C(\Delta\phi) = \frac{2\pi \int_{p_T, p_T^h > p_T^{\text{cut}}} dp_T p_T^h dp_T^h p_T^h \frac{d\sigma(pA \rightarrow hG^*X)}{dY dy_h d^2p_T d^2p_T^h}}{\int_{p_T > p_T^{\text{cut}}} dp_T p_T \frac{d\sigma(pA \rightarrow G^*X)}{dY d^2p_T}}, \quad (17)$$

where p_T^{cut} is the experimental low cut-off on transverse momenta of the resolved G^* (or dilepton) and a hadron h , $\Delta\phi$ is the angle between them. The differential cross sections entering the numerator and denominator of $C(\Delta\phi)$ have been derived for pp collisions in Ref. [12] taking into account both the γ^* and Z^0 boson contributions and can now be directly generalised for pA collisions by accounting the nuclear dependence of the saturation scale. We refer to Ref. [12] for details of the differential cross sections. As in Ref. [13], in what follows we study the correlation function $C(\Delta\phi)$ taking the unintegrated gluon distribution (UGDF) in the following form

$$F(x_g, k_T^g) = \frac{1}{\pi Q_{s,A}^2(x_g)} e^{-k_T^g{}^2/Q_{s,A}^2(x_g)}, \quad (18)$$

where x_g and k_T^g are the momentum fraction and transverse momentum of the target gluon, $Q_{s,A}^2(x) = A^{1/3}c(b)Q_{s,p}^2(x)$ is the saturation scale and $Q_{s,p}^2(x)$ is given by Eq. (14). In numerical analysis, the CT10 NLO parametrization [51] for the parton distributions and the Kniehl-Kramer-Potter (KKP) fragmentation function $D_{h/f}(z_h, \mu_F^2)$ of a quark to a neutral pion [56] have been used. Moreover, we assume that the minimal transverse momentum (p_T^{cut}) of the gauge boson G^* and the pion $h = \pi$ in Eq. (17) are the same and equal to 1.5 and 3.0 GeV for RHIC and LHC energies, respectively. As in our previous study [12], we assume that the factorisation scale is given by the dilepton invariant mass, i.e. $\mu_F = M_{l\bar{l}}$.

Considering our results for pp collisions [12], we have that the increasing of the saturation scale at large rapidities implies a larger value for the transverse momentum carried by the low- x gluons in the target which generates the

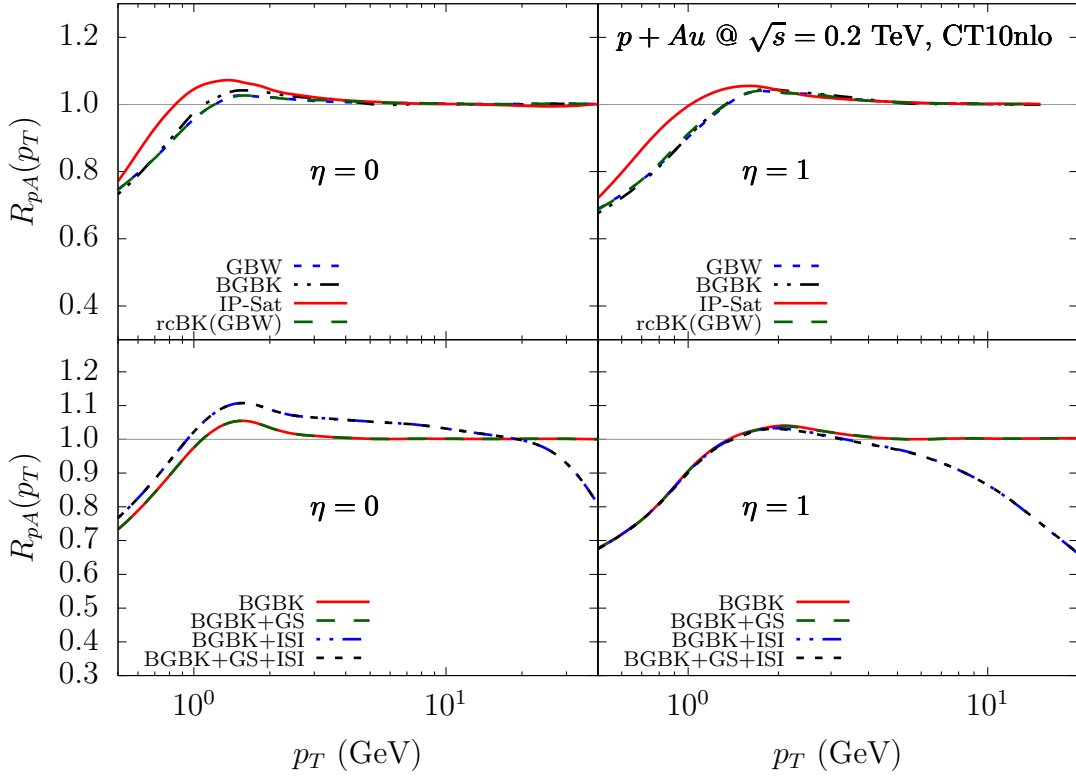


FIG. 7: (Color online) The transverse momentum dependence of the nucleus-to-nucleon ratio of the DY production cross sections, $R_{pA}(p_T)$, for the dilepton invariant mass range $5 < M_{l\bar{l}} < 25$ GeV at $\sqrt{s} = 0.2$ TeV and $\eta = 0, 1$.

decorrelation between the back-to-back jets. In the case of pA collisions, the magnitude of the saturation scale is amplified by the factor $A^{\frac{1}{3}}$. Consequently, we should also expect the presence a double-peak structure of $C(\Delta\phi)$ in the away side dilepton-pion angular correlation in pA collisions. This expectation is verified in our predictions presented in Fig. 10, where we show our predictions for the correlation function $C(\Delta\phi)$ of the associated DY pair and pion in pA collisions at LHC energies and different values of the atomic mass number. We have that larger values of A implies the smearing of the the back-to-back scattering pattern and suppress the away-side peak in the $\Delta\phi$ distribution. Our predictions for the RHIC and LHC kinematical regions are presented in Fig. 11, which agree with the results for small invariant masses presented in Refs. [12, 13]. In variance with our results for pp collisions [12], we also predict a double-peak structure for large invariant masses. This new result is directly associated with the larger value of the saturation scale present in pA collisions and to the fact that the typical momentum transverse of the produced particles is smaller in pA collisions at $\sqrt{s} = 5.02$ TeV than for pp collisions at $\sqrt{s} = 14$ TeV. As a consequence, the effect of the transverse momentum of the exchanged gluon is larger, implying the imbalance of the back-to-back jets also for large invariant masses in pA collisions, generating thus the double-peak structure observed in Fig. 11.

IV. SUMMARY

In this paper, we carried out an extensive phenomenological analysis of the inclusive DY $\gamma^*/Z^0 \rightarrow l\bar{l}$ process in pA collisions within the color dipole approach. At large dilepton invariant masses the Z^0 contribution becomes relevant. The corresponding predictions for the dilepton invariant mass and transverse momentum differential distributions have been compared with available data at the LHC and a reasonable agreement was found. The invariant mass, rapidity and transverse momentum dependencies of the nucleus-to-nucleon ratio of production cross sections, $R_{pA} = \sigma_{pA}^{DY} / (A \cdot \sigma_{pp}^{DY})$, were estimated taking into account such nuclear effects as the saturation, gluon shadowing GS and initial state energy loss effects (ISI effects).

In comparison with other processes with inclusive particle production, the DY reaction is very effective tool for study of nuclear effects since no final state interaction is expected, either the energy loss or absorption. For this reason the DY process represents a cleaner probe for the medium created not only in pA interactions but also in

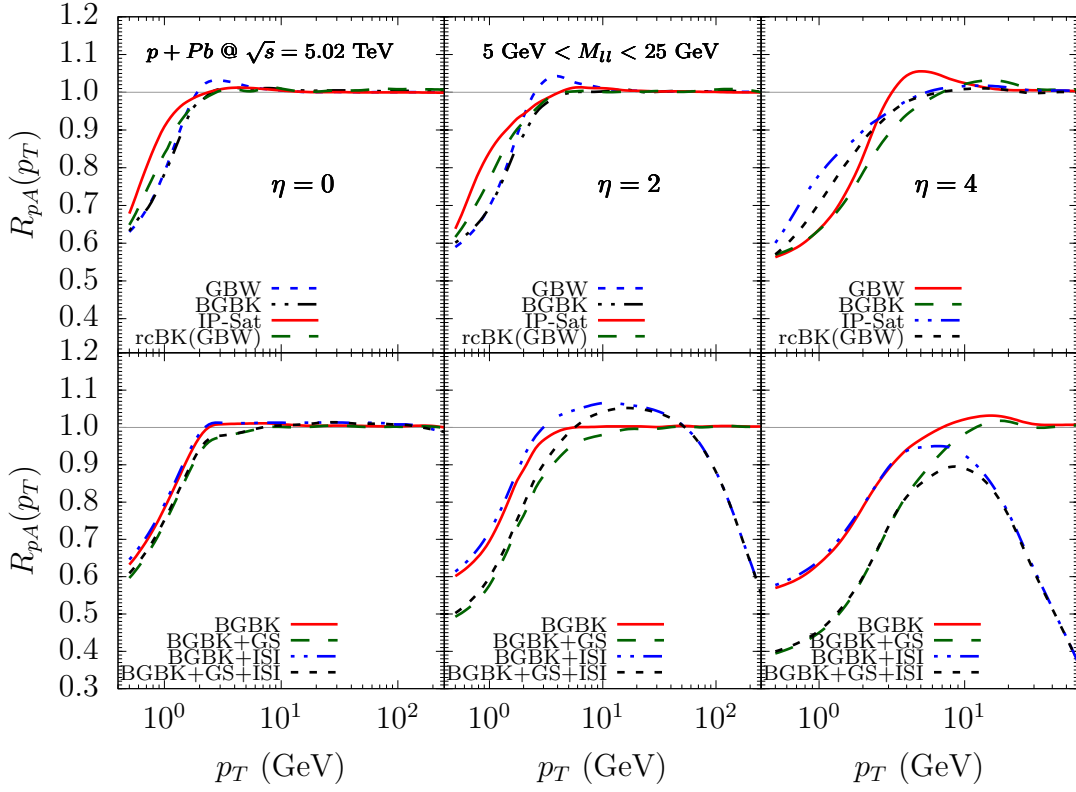


FIG. 8: (Color online) The transverse momentum dependence of the nucleus-to-nucleon ratio of the DY production cross sections, $R_{pA}(p_T)$, for the dilepton invariant mass range $5 < M_{l\bar{l}} < 25$ GeV at $\sqrt{s} = 5.02$ TeV and $\eta = 0, 2, 4$.

heavy ion collisions. Our results demonstrate that the analysis of the DY process off nuclei in different kinematic regions allows us to investigate the magnitude of particular nuclear effects. We found that both GS and ISI effects cause a significant suppression in DY production. Whereas GS effects dominate at small Bjorken- x in the target the ISI effects (in accordance with Eq. (16)) become effective at large transverse momenta p_T and invariant masses $M_{l\bar{l}}$ of dilepton pairs as well as at large Feynman x_F (forward rapidities). Consequently, at forward rapidities in some kinematic regions at the LHC one can investigate only a mixing of both effects even at large p_T - values. However, in contrast to other inclusive processes, the advantage of the DY reaction arises in elimination of the GS-ISI mixing by elimination of coherence effects going to larger values of the dilepton invariant mass. Then an investigation of nuclear suppression at large p_T represents a clear manifestation of net ISI effects even at forward rapidities as is demonstrated in Fig. 9. Such a study of nuclear suppression at large dilepton invariant masses, transverse momenta and rapidities especially at the LHC energy favours the DY process as an effective tool for investigation of net ISI effects.

Besides, we have analysed the correlation function $C(\Delta\phi)$ in azimuthal angle $\Delta\phi$ between the produced dilepton and a forward pion, which results by a fragmentation from a projectile quark radiating the virtual gauge boson. The corresponding observable has been studied at various energies in pA collisions in both the low and high dilepton invariant mass ranges as well as at different rapidities of final states. We found a characteristic double-peak structure of the correlation function around $\Delta\phi \simeq \pi$ at various dilepton mass values and for a very forward pion. The considering observable is more exclusive than the ordinary DY process. Such a measurement at different energies at RHIC and LHC is therefore capable of setting further even stronger constraints on saturation physics.

Acknowledgements

E.B. is supported by CAPES and CNPq (Brazil), contract numbers 2362/13-9 and 150674/2015-5. V.P.G. has been supported by CNPq, CAPES and FAPERGS, Brazil. R.P. is supported by the Swedish Research Council, contract number 621-2013-428. J.N. and M.K. are partially supported by the grant 13-02841S of the Czech Science Foundation (GAČR) and by the Grant MŠMT LG15001. J.N. is supported by the Slovak Research and Development Agency

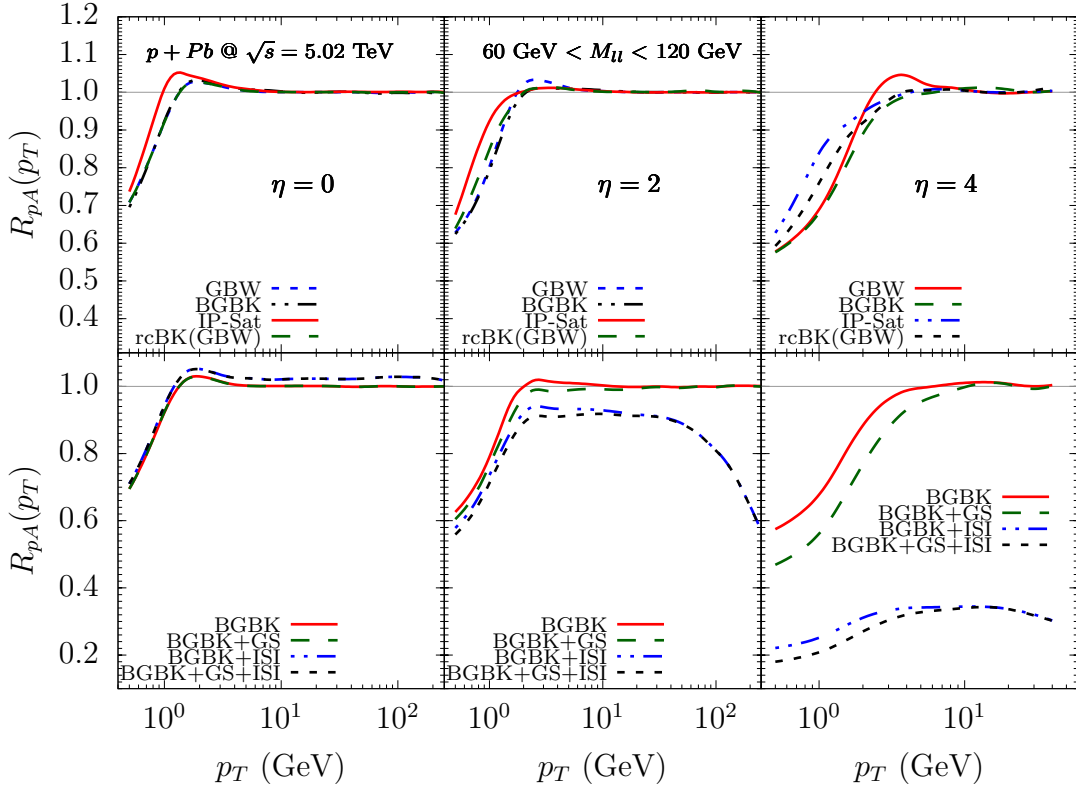


FIG. 9: (Color online) The transverse momentum dependence of the nucleus-to-nucleon ratio of the DY production cross sections, $R_{pA}(p_T)$, for the dilepton invariant mass range $60 < M_{ll} < 120$ GeV at $\sqrt{s} = 5.02$ TeV and $\eta = 0, 2, 4$.

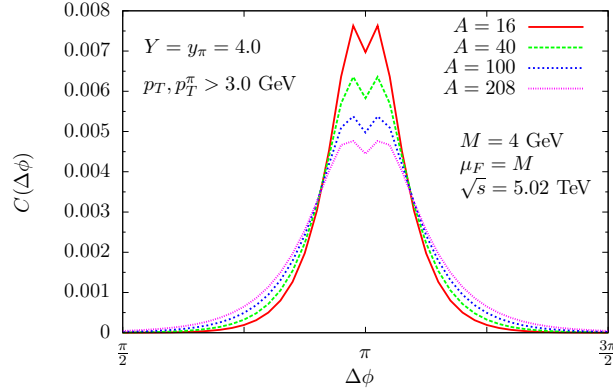


FIG. 10: (Color online) The correlation function $C(\Delta\phi)$ for the associated DY pair and pion production in pA collisions at the LHC ($\sqrt{s} = 5.02$ TeV) for different mass numbers A .

APVV-0050-11 and by the Slovak Funding Agency, Grant 2/0020/14.

-
- [1] C.A. Salgado *et al.*, J. Phys. **G39**, 015010 (2012).
 [2] J.C. Peng and J.W. Qiu, Prog. Part. Nucl. Phys. **76**, 43 (2014).
 [3] B.Z. Kopeliovich, in *Proceedings of the international workshop XXIII on Gross Properties of Nuclei and Nuclear Excitations, Hirschegg, Austria, 1995*, edited by H. Feldmeyer and W. Nörenberg (Gesellschaft Schwerionenforschung, Darmstadt, 1995),

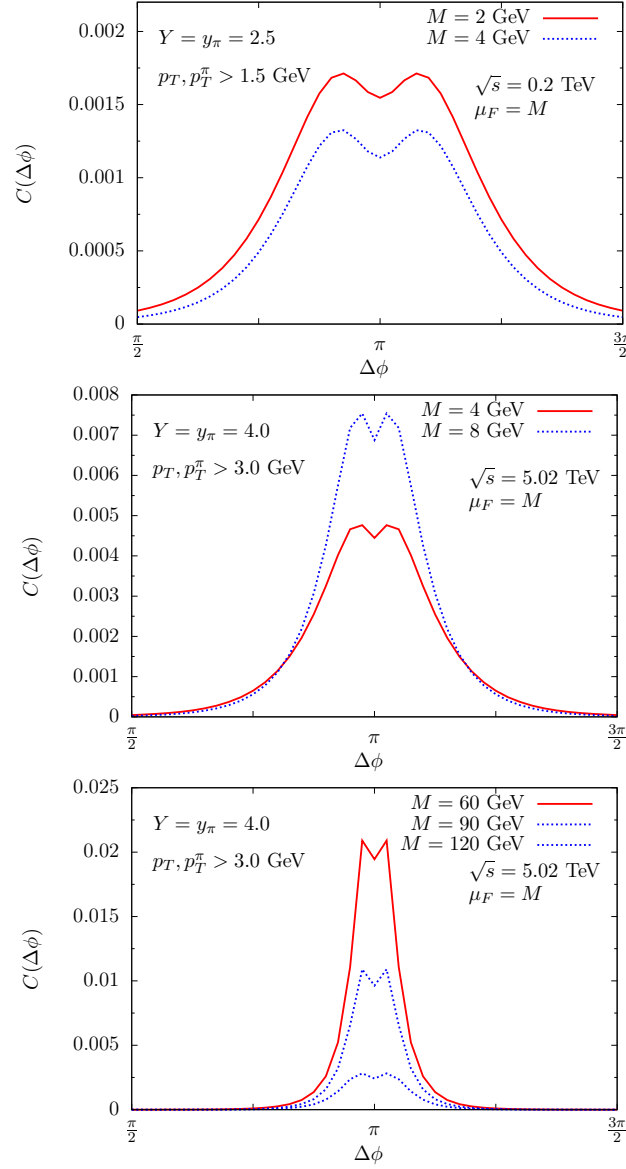


FIG. 11: (Color online) The correlation function $C(\Delta\phi)$ for the associated DY pair and pion production in pA collisions at RHIC ($\sqrt{s} = 0.2$ TeV) and LHC ($\sqrt{s} = 5.02$ TeV) energies and different values of the dilepton invariant mass.

p. 385.

- [4] S.J. Brodsky, A. Hebecker and E. Quack, Phys. Rev. D**55**, 2584 (1997).
- [5] B.Z. Kopeliovich, A. Schafer, and A.V. Tarasov, Phys. Rev. C**59**, 1609 (1999).
- [6] B.Z. Kopeliovich, J. Raufeisen, and A.V. Tarasov, Phys. Lett. B**503**, 91 (2001).
- [7] B.Z. Kopeliovich, J. Raufeisen, A.V. Tarasov and M.B. Johnson, Phys. Rev. C**67**, 014903 (2003).
- [8] J. Raufeisen, J.C. Peng and G.C. Nayak, Phys. Rev. D**66**, 034024 (2002);
M.B. Johnson, B.Z. Kopeliovich, M.J. Leitch, P.L. McGaughey, J.M. Moss, I.K. Potashnikova and I. Schmidt, Phys. Rev. C**75**, 035206 (2007);
M.B. Johnson, B.Z. Kopeliovich and I. Schmidt, Phys. Rev. C**75**, 064905 (2007).
- [9] M.A. Betemps, M.B.G. Ducati and M.V.T. Machado, Phys. Rev. D**66**, 014018 (2002);
M.A. Betemps, M.B.G. Ducati, M.V.T. Machado and J. Raufeisen, Phys. Rev. D**67**, 114008 (2003);
M.A. Betemps and M.B.G. Ducati, Phys. Rev. D**70**, 116005 (2004); Phys. Lett. B**636**, 46 (2006);
M.A. Betemps, M.B.G. Ducati and E.G. de Oliveira, Phys. Rev. D**74**, 094010 (2006);
M.B.G. Ducati and E.G. de Oliveira, Phys. Rev. D**81**, 054015 (2010);
M.B.G. Ducati, M.T. Griep and M.V.T. Machado, Phys. Rev. D**89**, 034022 (2014).

- [10] R.S. Pasechnik, B.Z. Kopeliovich, and I.K. Potashnikova, Phys. Rev. D**86**, 114039 (2012).
- [11] E.A.F. Basso, V.P. Goncalves and M. Rangel, Phys. Rev. D**90**, 094025 (2014).
- [12] E. Basso, V.P. Goncalves, J. Nemchik, R. Pasechnik and M. Sumnera, Phys. Rev. D**93**, 034023 (2016).
- [13] A. Stasto, B-W Xiao and D. Zaslavsky, Phys. Rev. D**86**, 014009 (2012).
- [14] F. Gelis, E. Iancu, J. Jalilian-Marian and R. Venugopalan, Ann. Rev. Nucl. Part. Sci. **60**, 463 (2010);
E. Iancu and R. Venugopalan, arXiv:hep-ph/0303204;
H. Weigert, Prog. Part. Nucl. Phys. **55**, 461 (2005);
J. Jalilian-Marian and Y.V. Kovchegov, Prog. Part. Nucl. Phys. **56**, 104 (2006);
J.L. Albacete and C. Marquet, Prog. Part. Nucl. Phys. **76**, 1 (2014).
- [15] J. Jalilian-Marian, A. Kovner, L. McLerran and H. Weigert, Phys. Rev. D**55**, 5414 (1997);
J. Jalilian-Marian, A. Kovner and H. Weigert, Phys. Rev. D**59**, 014014 (1999), *ibid.* **59**, 014015 (1999), *ibid.* **59** 034007 (1999);
A. Kovner, J. Guilherme Milhano and H. Weigert, Phys. Rev. D**62**, 114005 (2000);
H. Weigert, Nucl. Phys. A**703**, 823 (2002);
E. Iancu, A. Leonidov and L. McLerran, Nucl. Phys. A**692**, 583 (2001);
E. Ferreira, E. Iancu, A. Leonidov and L. McLerran, Nucl. Phys. A**701**, 489 (2002).
- [16] I.I. Balitsky, Phys. Rev. Lett. **81**, 2024 (1998); Phys. Lett. B**518**, 235 (2001);
I.I. Balitsky and A.V. Belitsky, Nucl. Phys. B**629**, 290 (2002).
- [17] Y.V. Kovchegov, Phys. Rev. D**60**, 034008 (1999); Phys. Rev. D**61**, 074018 (2000).
- [18] K.J. Golec-Biernat and A.M. Stasto, Nucl. Phys. B**668**, 345 (2003);
J. Berger and A. Stasto, Phys. Rev. D**83**, 034015 (2011); Phys. Rev. D**84**, 094022 (2011).
- [19] E.R. Cazaroto, F. Carvalho, V.P. Goncalves and F.S. Navarra, Phys. Lett. B**671**, 233 (2009).
- [20] V.P. Goncalves, M.S. Kugeratski, M.V.T. Machado and F.S. Navarra, Phys. Rev. C**80**, 025202 (2009).
- [21] E.R. Cazaroto, F. Carvalho, V.P. Goncalves, M.S. Kugeratski and F.S. Navarra, Phys. Lett. B**696**, 473 (2011).
- [22] F. Carvalho, V.P. Goncalves, F.S. Navarra and E.G. de Oliveira, Phys. Rev. C**87**, 065205 (2013).
- [23] V.P. Goncalves and D.S. Pires, Phys. Rev. C**91**, 055207 (2015).
- [24] V.P. Goncalves, F.S. Navarra and D. Spiering, arXiv:1510.01512 [hep-ph].
- [25] B.Z. Kopeliovich, L.I. Lapidus, A.B. Zamolodchikov, JETP Lett. **33**, 595-597 (1981).
- [26] N. Armesto, Eur. Phys. J. C**26**, 35 (2002).
- [27] H.De Vries, C.W.De Jager and C.De Vries, Atomic Data and Nucl. Data Tables **36**, 469 (1987).
- [28] V.N. Gribov, Sov. Phys. JETP **30**, 709 (1970) [Zh. Eksp. Teor. Fiz. **57**, 1306 (1969)].
- [29] K.J. Golec-Biernat, M. Wusthoff, Phys. Rev. D**59**, 014017 (1998).
- [30] E. Iancu, K. Itakura, S. Munier, Phys. Lett. B**590**, 199 (2004).
- [31] D. Kharzeev, Y.V. Kovchegov and K. Tuchin, Phys. Lett. B**599**, 23 (2004).
- [32] A. Dumitru, A. Hayashigaki and J. Jalilian-Marian, Nucl. Phys. A**765**, 464 (2006).
- [33] V.P. Goncalves, M.S. Kugeratski, M.V.T. Machado and F.S. Navarra, Phys. Lett. B**643**, 273 (2006).
- [34] D. Boer, A. Utermann, E. Wessels, Phys. Rev. D**77**, 054014 (2008).
- [35] H. Kowalski, L. Motyka and G. Watt, Phys. Rev. D**74**, 074016 (2006);
G. Watt and H. Kowalski, Phys. Rev. D**78**, 014016 (2008).
- [36] J.T. de Santana Amaral, M.B. Gay Ducati, M.A. Betemps, and G. Soyez, Phys. Rev. D**76**, 094018 (2007);
E.A.F. Basso, M.B.G. Ducati and E.G. de Oliveira, Phys. Rev. D**87**, 074023 (2013).
- [37] G.Soyez, Phys. Lett. B**655**, 32 (2007).
- [38] J. Bartels, K. Golec-Biernat, and H. Kowalski, Phys. Rev. D**66**, 014001 (2002).
- [39] H. Kowalski and D. Teaney, Phys. Rev. D**68**, 114005 (2003).
- [40] A.H. Rezaeian, M. Siddikov, M. Van de Klundert and R. Venugopalan, Phys. Rev. D**87**, 034002 (2013).
- [41] A. Rezaeian and I. Schmidt, Phys. Rev. D**88**, 074016 (2013).
- [42] V.N. Gribov and L.N. Lipatov, Sov. J. Nucl. Phys. **15**, 438 (1972);
G. Altarelli and G. Parisi, Nucl. Phys. B**126**, 298 (1977);
Yu.L. Dokshitzer, Sov. Phys. JETP **46**, 641 (1977).
- [43] F.D. Aaron *et al.* [H1 and ZEUS Collaborations], JHEP **1001**, 109 (2010);
H. Abramowicz *et al.* [H1 and ZEUS Collaborations], Eur. Phys. J. C**73** 2311 (2013).
- [44] J.L. Albacete, N. Armesto, J.G. Milhano and C.A. Salgado, Phys. Rev. D**80**, 034031 (2009).
- [45] B.Z. Kopeliovich, A. Schaefer, and A.V. Tarasov, Phys. Rev. D**62**, 054022 (2000);
B.Z. Kopeliovich, J. Nemchik, A. Schaefer, Phys. Rev. C**65**, 035201 (2002);
B.Z. Kopeliovich, J. Nemchik, I.K. Potashnikova, I. Schmidt, J. Phys. G**35**, 115010 (2008).
- [46] D. de Florian and R. Sassot, Phys. Rev. D**69**, 074028 (2004);
M. Hirai, S. Kumano and T.H. Nagai, Phys. Rev. C**70**, 044905 (2004).
- [47] B.Z. Kopeliovich, J. Nemchik, I.K. Potashnikova, M.B. Johnson, I. Schmidt, Phys. Rev. C**72**, 054066 (2005);
B.Z. Kopeliovich, J. Nemchik, I.K. Potashnikova, I. Schmidt, Int. J. Mod. Phys. E**23**, 1430006 (2014).
- [48] S.S. Adler *et al.* [PHENIX Collab.], Phys. Rev. Lett. **98**, 172302 (2007);
Phys. Rev. Lett. **109**, 152302 (2012).
- [49] S. Afanasiev *et al.* [PHENIX Collab.], Phys. Rev. Lett. **109**, 152302 (2012);
T. Sakaguchi, Nucl. Phys. A**805**, 355 (2008).
- [50] I. Arsene *et al.* [BRAHMS Collab.], Phys. Rev. Lett. **93**, 242303 (2004);

- J. Adams *et al.* [STAR Collab.], Phys. Rev. Lett. **97**, 152302 (2006).
- [51] H.L. Lai, M. Guzzi, J. Huston, Z. Li, P.M. Nadolsky, J. Pumplin and C.P. Yuan, Phys. Rev. D**82**, 074024 (2010).
- [52] E. Basso, C. Bourrely, R. Pasechnik and J. Soffer, arXiv:1509.07988 [hep-ph].
- [53] V. Khachatryan *et al.* [CMS Collaboration], arXiv:1512.06461 [hep-ex].
- [54] G. Aad *et al.* [ATLAS Collaboration], Phys. Rev. C**92**, 044915 (2015).
- [55] J. Jalilian-Marian and A.H. Rezaeian, Phys. Rev. D**86**, 034016 (2012);
A.H. Rezaeian, Phys. Rev. D**86**, 094016 (2012).
- [56] B.A. Kniehl, G. Kramer and B. Potter, Nucl. Phys. B**582**, 514 (2000).